A structural study of poly(*p*-phenylene vinylene)

Dong Chen and M. J. Winokur*
Department of Physics, University of Wisconsin, Madison, WI 53706, USA

and M. A. Masse† and Frank E. Karasz
Department of Polymer Science & Engineering, University of Massachusetts, Amherst, MA 01003, USA
(Received 15 December 1990; revised 22 August 1991; accepted 9 September 1991)

X-ray diffraction profiles of highly oriented poly(*p*-phenylene vinylene) (PPV) samples have been acquired at temperatures ranging from 20 to 700 K. The resulting equatorial data have been analysed using a linked-atom-least-square structure factor refinement algorithm that allows for a more complete characterization of the polymer structure and of its temperature-dependent evolution. The resulting analysis identifies strong librational motions of the phenyl rings, a finding in agreement with recent n.m.r. studies. In additon, thin films of PPV are found to possess measurable equatorial anisotropy with [200] and [110] lattice planes preferentially oriented parallel to the film surface.

(Keywords: structural properties; poly(*p*-phenylene vinylene); conducting polymers; X-ray diffraction)

INTRODUCTION

Conducting polymer synthesis via soluble precursor polymers[1–3] has become an established method for preparing high-quality films with excellent material properties[4]. In particular, poly(*p*-phenylene vinylene) (PPV) films fabricated in this manner are especially well-suited for diffraction studies because they can exhibit a high degree of crystallinity and relatively large coherence lengths[5,6]. These attributes initially develop during the simultaneous thermal conversion and uniaxial stretching of the precursor films and can be further enhanced by additional heat treatment[7,8]. As a result of these properties and the comparative ease with which PPV films may be prepared, PPV is considered a prototypical non-degenerate ground-state conducting polymer host.

Previous studies have identified the basic structural features inherent to pristine PPV films[5,6,9–11]. Fully dense films can be fabricated and these films nominally exhibit a smooth lamellar morphology. On a smaller scale, there is a microfibrillar construction of crystallites that are embedded in less-ordered grain boundary regions[12]. Within individual PPV crystallites the lateral packing of the polymer chains is very regular and there is a herringbone arrangement of the polymer units with two chains per projected two-dimensional rectangular unit cell (*p2gg* symmetry), as shown in *Figure 1a*. Both electron and X-ray diffraction measurements yield similar lattice spacings. The overall organization of PPV can be referenced to a monoclinic unit cell with nominal lattice parameters of $a = 0.80$ nm, $b = 0.60$ nm, c(chain axis) = 0.66 nm and $\alpha = 123°$. Additionally, Granier *et al.*[9] have performed structural refinements of the equatorial profiles and determined that the setting angle ϕ_s (the angular position of the projected molecular major axis with respect to the a-axis direction) lies somewhere between 56° and 68°. A more recent result[11] quotes a value of 52°. The precise three-dimensional structure is quite complex for there are noticeable axial registration fluctuations of the polymer chains. This disorder generates pronounced layer-line streaking of the non-equatorial reflections and the associated displacement tensors have been deduced[10].

In this paper we summarize an extensive study of the PPV equatorial structure. These results are nominally in agreement with those of Granier *et al.*[9] but we obtain significantly better structural refinements. Most samples can be adequately modelled by the aforementioned structure but detailed comparisons of the refinements with experimental data show statistically significant departures and, for a few samples, there are pronounced deviations from this model. We also observe substantial equatorial anisotropy in extremely thin ($\leqslant 3\ \mu$m) PPV films that have been processed with a web-stretching device. For these PPV films, the microscopic crystallite distribution has been characterized. Furthermore, we observe that subsequent doping of these films with sodium vapour does not appreciably alter this anisotropy. Finally, new results on the temperature dependence of the equatorial structure are presented that suggest that PPV has a non-planar conformation of the individual polymer chains combined with strong librational motions of the phenyl rings about the C–C vinyl linkages.

*To whom correspondence should be addressed
†Present address: Shell Development Company, Westhollow Research Center, PO Box 1380, Houston, TX 77215, USA

0032-3861/92/153116-07

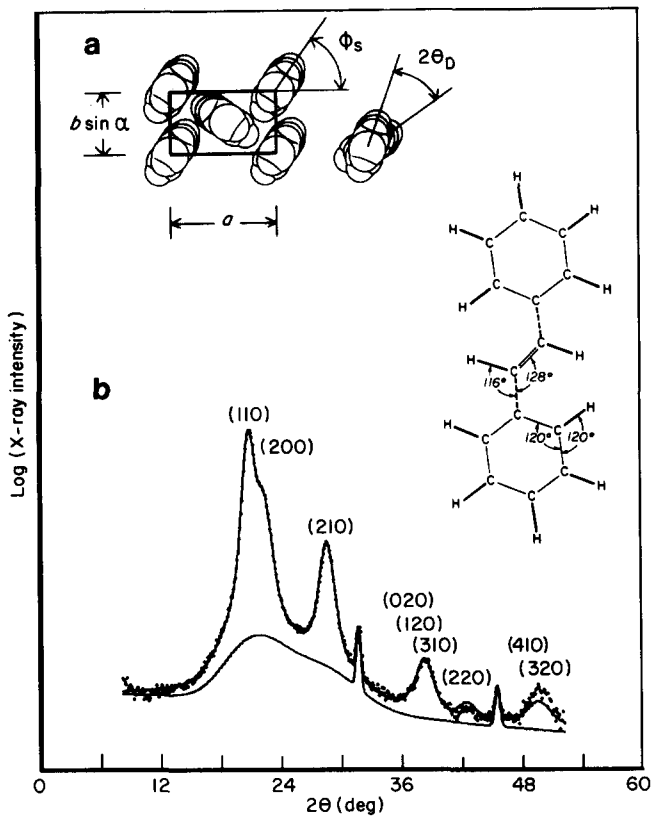

Figure 1 (a) Upper left: the proposed equatorial PPV unit cell structure of reference 9. Middle right: a model of planar *trans*-stilbene according to reference 15. (b) Comparison of the experimental (*hk*0) diffraction profile (●) with the best fit obtained by structure factor calculations (——). The background profile (including corrections for NaCl residues at 31.9° and 45.5°) is shown at the bottom. (Note the log scale)

EXPERIMENTAL

Thin PPV films were obtained by thermal conversion of the precursor polymer[13] poly(*p*-xylene-α-dimethylsulphonium chloride). During conversion to PPV, the precursor films were passed over heated rollers in a uniaxial web stretching device[14] to final draw ratios of ~10:1. These films were subsequently annealed under dynamic vacuum at 300°C for ~4 h. This processing resulted in highly oriented polymer films with a *c*-axis mosaic of typically < 7° (as determined from the angular widths at half-maximum of equatorial reflections).

For study, PPV film strips (~1.5 mm wide) were carefully folded and clamped to maintain their preferential orientation. The overall multilayer film thicknesses varied but were typically < 200 μm. For the elevated temperature stydies, the polymer films were loaded into argon-filled X-ray glass capillaries and mounted into a home-built furnace with beryllium windows. For reduced temperatures, the films were attached to the cold-finger of a closed-cycle helium cryostat (Cryomech GB-15).

Structural studies were performed using Cu Kα (1.542 Å) radiation from a rotating-anode X-ray generator (Elliot GX-21) fitted with a bent-graphite crystal monochromator. All samples were placed in a four-circle diffractometer (Huber series 410). Diffractometer scans were executed with the diffraction vector in the equatorial *a**-*b** plane of the polymer (orthogonal to the *c*-axis) and thus only (*hk*0) reflections were monitored. The diffracted X-rays were detected by a small linear silicon-diode array detector (EG&G model 1412XR) that was mounted to the 2θ arm of the diffractometer. Details of this experimental set-up have been discussed elsewhere[11]. In general, a collimated 1.5 × 1.5 mm^2 X-ray beam incident on a typical sample gave a total count rate exceeding 1000 counts s^{-1} for the most intense scattering features.

STRUCTURAL REFINEMENTS

To perform these structure factor calculations, a linked-atom-least-square algorithm[15] was used whereby the calculated diffraction profiles, including standard crystallographic corrections, were scaled and compared directly with the experimental data. Using this method the unit cell dimensions could be treated as adjustable parameters so that all aspects of the best-fit profile could be assessed within a single fitting procedure. In addition to the standard temperature factors, these calculations also included a variable that parameterized librational ring motions. Since very few isolated (*hk*0) reflections were resolvable, a superposition of peaks was first fit directly to the experimental data in order to ascertain individual peak widths and heights prior to structure factor refinement.

For the PPV coordinates, bond angle and bond lengths were initially established using the refined parameters of stilbene molecular crystals as reported by Finder *et al.*[16]. In our structure factor calculations, both the carbon bond angles within the vinyl linkage (see *Figure 1a*) and the dihedral angle, θ_D, formed by the plane of the phenyl ring and that of the vinyl segment, were considered as adjustable parameters. Stilbene possesses bond angles of 116° and 128° and a θ_D of 3–5°. This latter degree of freedom indicates a deviation from planarity and its origin can be traced to the repulsive interaction between the vinyl hydrogen and the α hydrogen of the phenyl group. The analogous situation is quite pronounced in the poly(*p*-phenylene) family of oligomers and mediates a sequence of structural transformations[17].

The data in *Figure 1b* show a comparison of the calculated equatorial (*hk*0) and experimental profiles for one PPV sample. The individual *d*-spacings and intensities for this sample are listed in *Table 1*. The calculated reliability factor for this sample, $R = 0.01$, is substantially less than that of Granier *et al.*[9] using the expression:

$$R = \frac{\sum_{hk0} [|F_{hk0}^{obs.}| - |F_{hk0}^{calc.}|]}{\sum_{hk0} |F_{hk0}^{obs.}|} \quad (1)$$

where $F_{hk0}^{obs.}$ and $F_{hk0}^{calc.}$ are the observed and calculated structure factor moduli, respectively. For most samples our calculated reliability factors are at least a factor of 5 smaller. A direct comparison to the result of Granier *et al.*[9] must be tempered somewhat due to the subjective nature of choosing the appropriate background profile (*Figure 1*) and by the introduction of additional free parameters in the structure factor refinements. For this work θ – 2θ scans with the equatorial (*hk*0) plane of the sample tilted some 20° to the scattering plane of the detector were used to establish an initial background baseline. Then small, systematic failings of this background profile were eliminated by introducing additional corrections. In particular, we note that

Table 1 Structure factor moduli and d-spacings for the sample in *Figure 1*

hkl	$\|F\|_{calc.}$	$\|F\|_{obs.}$	$d_{calc.}$ (nm)	$d_{obs.}$ (nm)
110	45.2	46.2	0.425	0.424
200	30.8	28.6	0.398	0.397
210	23.6	23.1	0.312	0.312
020	1.1	2.2	0.251	0.252
120	5.6	4.5	0.239	0.239
310	9.3	10.1	0.235	0.234
220	4.6	4.0	0.212	0.212
400	0.9	0.0	0.199	–
320	4.9	6.3	0.182	0.184
410	4.5	6.3	0.185	0.184

$R = 0.01$ using equation (1) and $\phi_s = 50 \pm 2°$ for this sample

virtually all samples exhibit a small shoulder (of undetermined origin) on the low-angle side of the (110) reflection.

Most samples gave similar results. All observed peak lineshapes were best described by a linear combination of Lorentzian and Gaussian profiles. As expected there was some variance in the projected two-dimensional lattice constants with deviations on the order of 1%. These refinements also fix the setting angle of this sample at $50 \pm 2°$ with a sample-to-sample standard deviation, $\sigma_{\phi_s} \sim 2°$. The relative (110)/(200) intensity ratio is particularly sensitive to this setting angle. This result is significantly less than the previously cited value and is more precisely determined. This value of ϕ_s brings nearest-neighbour interchain C–C, C–H and H–H contact distances, for a (001) projection of the chains, close to 0.33, 0.23 and 0.21 nm, respectively.

Adjustments in the previously defined θ_D affected the calculated structure factors slightly, a result qualitatively consistent with the findings of Granier *et al.*[9]. Smaller θ_D settings required a simultaneous compensating increase in the calculated Debye temperature factor. While this behaviour was not an unreasonable complication for room temperature scans, elevated temperature studies (see later) suggest that a non-planar conformation is present in pristine PPV. In general, the best fits required θ_D values of 8–16°. For the sample in *Table 1* the best fit θ_D is found to be $10 \pm 3°$. The calculated profile fits were also found to improve upon increasing the vinyl linkage bond angles by 2°. This latter process would be a natural response if PPV were to adopt a planar conformation, for this relaxation would partially offset the repulsive intrachain hydrogen interaction. The best-fit isotropic Debye temperature coefficients of our refinements were always near 0.12 ± 0.02 nm^2 and are considerably less than the previous estimate of 0.20 nm^2 by Granier *et al.*[9]. For samples annealed at 300°C, the estimated crystallite size was 10 nm.

By performing a high-temperature anneal at 400°C, substantial improvements in the experimental diffraction profiles could be achieved. For the annealed sample shown in *Figure 2A*, the maximum peak intensity increased by 30% and all ($hk0$) peaks narrowed noticeably [e.g. the (110) and (200) peaks are clearly distinguishable]. The final room temperature two-dimensional lattice parameters for this sample were $a = 0.793 \pm 0.003$ nm, $b \sin \alpha = 0.503 \pm 0.002$ nm and $\phi_s = 49 \pm 2°$ with the lattice spacings reduced ~0.5% from their initial values prior to this annealing. The calculated reliability factor, R, for this sample was 0.03.

The improved resolution of the individual equatorial reflections simplifies analysis of the peak-width variations. For ($hk0$) reflections there should be gradual increases, upon increasing scattering angle, resulting from the Debye–Scherrer relationship and from the presence of various disorder effects[18,19]. The most likely source of this disorder are microstrains arising from conformational chain defects and the persistence of precursor polymer side group residues. In general, we find that the progressive peak width increases are beyond the functional dependence of the Debye–Scherrer relationship even for samples annealed at the highest temperatures. Extrapolating to zero degrees results in an estimated equatorial coherence length exceeding 14 nm. We also note that while annealing clearly enhances the crystallographic properties of PPV, these high temperatures could effectively reduce the overall conjugation length[5]. Additionally, this improved crystallinity may also lead to even poorer dopant-ion diffusion properties.

Although the total number of crystallographically distinct reflections is small (~8), the topology of the structure factor refinement surface is surprisingly complex with the presence of shallow local minima. This complexity can be traced to systematic shortcomings in this model to simultaneously fit all of the experimental reflections to within statistical limits. Moreover, the reliability factor in equation (1) strongly weights the most intense reflections, and, hence, the fits to the weaker reflections at higher angles suffer most. For all samples encountered, the best-fit parameter consistently underestimated the intensity of the (020), (120), (310) and the (410), (320) peak superpositions while simultaneously overestimating the intensity of the (220) reflection. A

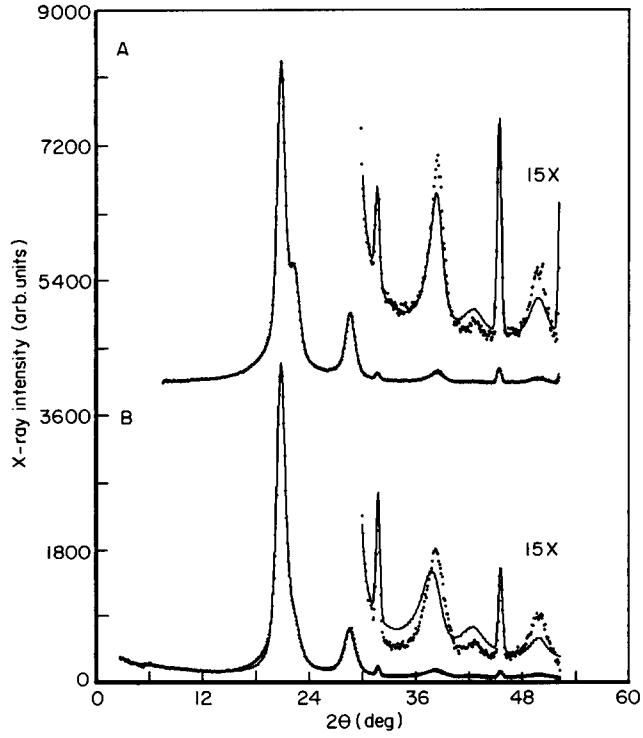

Figure 2 Comparison of the experimental ($hk0$) diffraction profiles (●) with the best fit obtained by structure factor calculations (——) for a sample annealed at 400°C (A) and for a sample with unusually small $\phi_s \sim 40°$ (B)

variety of structural modifications were investigated, but none was found that could improve upon the currently proposed model. Unfortunately, the limited number of clearly distinguishable equatorial reflections precludes a Patterson-map analysis along the lines of a recent polyethylene study by Busing[20].

A few samples exhibited extremely unusual diffraction profiles with an abnormally weak intensity of the (200) reflection (the high-angle shoulder on the 110 peak). A representative equatorial scan is displayed in *Figure 2B*. As a result, structure factor calculations yielded extraordinarily small setting angles of $\sim 40°$ and R values exceeding 0.1. While these fits are not altogether unreasonable, they suggest the possibility of additional structural phases in PPV films.

EQUATORIAL ANISOTROPY

Uniaxial processing of polymer films typically orients the c-axis (or the polymer chain axis) of the crystallites parallel to the stretching direction. For polymers[18] (or metals), rigorous mechanical processing can often lead to a full three-dimensional texturing of the host with subsequent modification in the bulk physical properties[21]. Presently there are few reports of these effects in synthesized and/or processed films of these highly conjugated compounds[22] although other rigid-rod polymers[23] are observed to manifest this behaviour. In fact, PPV films examined previously are reported to contain no measurable equatorial anisotropy.

Among the various samples investigated in the course of this study, the thinnest films (typically $\leqslant 3\ \mu m$) exhibited modest equatorial anisotropy. The results presented here are for a 64-layer stacked film of PPV with net dimensions of $0.2 \times 1.5 \times 3\ mm^3$. This film was mounted with its c-axis normal to the diffraction plane, and radial $\theta - 2\theta$ scans were acquired for every 15° (referred to as χ) rotation about the c-axis (see *Figure 3* inset). The equatorial plane could then be imaged by reconstructing a map of constant intensity contours using this data.

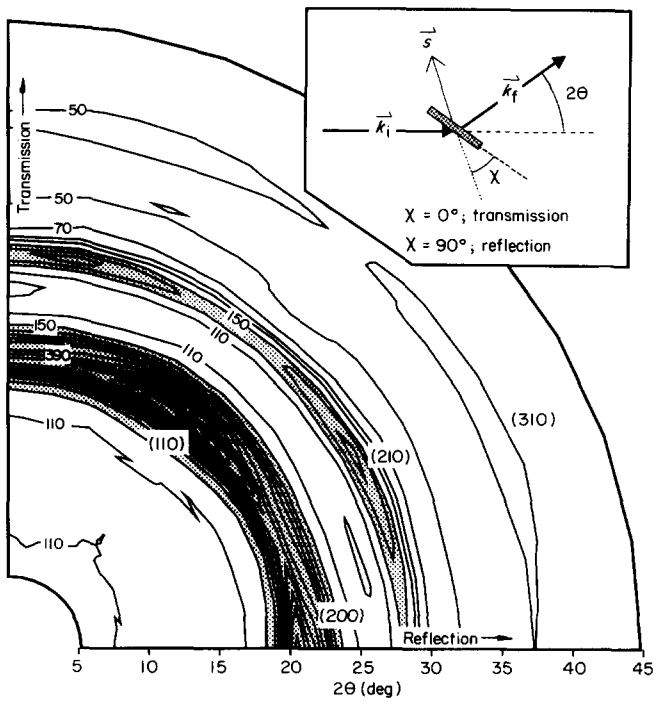

Figure 3 Constant X-ray intensity contour maps for the ($hk0$) equatorial plane of three-dimensional textured PPV films when undoped. Inset: sample scattering geometry. $\vec{k}_i$ and $\vec{k}_f$ are the incident and scattered wavevectors so that the scattering vector is given by $\vec{s} = \vec{k}_f - \vec{k}_i$ subject to the Bragg condition $|\vec{s}| = 4\pi \sin\theta/\lambda$. When χ is zero, the scattering vector is along the surface parallel and perpendicular to the polymer c-axis (transmission geometry). For χ at 90°, the scattering vector is along the surface normal and again perpendicular to the c-axis (reflection geometry)

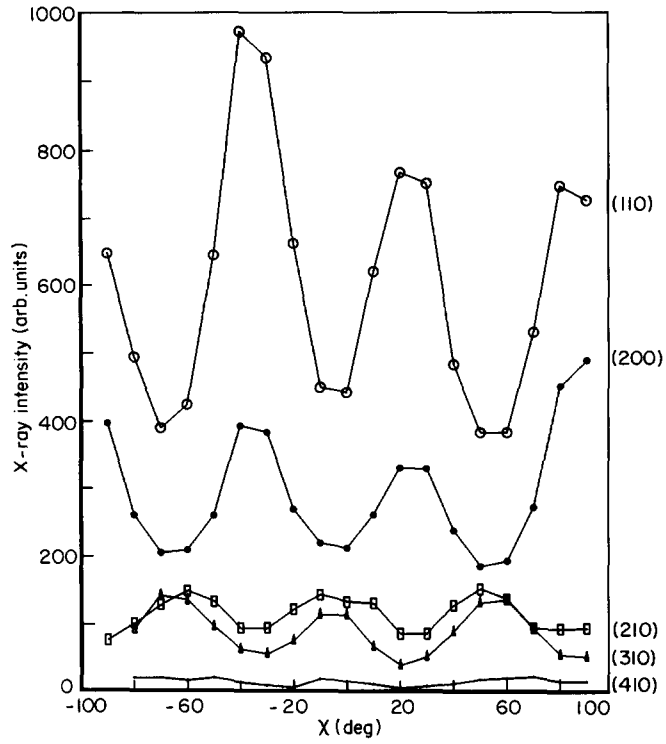

Figure 4 Equatorial angular anisotropy of various individually resolved ($hk0$) reflections. The asymmetry about $\chi = 0$ is an artifact due to slight sample misalignment. For clarity, both the (110) and (200) profiles have been shifted upwards by 100 counts

Figure 3 displays a mapping of the equatorial scattering plane, from transmission to reflection geometry, for this thin-film PPV sample. The presence of equatorial anisotropy is qualitatively evidenced by the strong angular variations (about χ) of the observed scattering signal at fixed 2θ. As a result of the finite radial peak widths, individual ($hk0$)s are not immediately resolved. By fitting every radial $\theta - 2\theta$ scan to a multiple peak superposition, individual equatorial ($hk0$) peaks could be distinguished. The results of this analysis for these reflections are shown in *Figure 4* and from this data it is evident that this anisotropy is moderately complex.

The overall interpretation can be simplifed by noting that the *p2gg* symmetry of the (001) projection of the PPV unit cell imparts a two-fold degeneracy to ($h00$) and ($0k0$) reflections and four-fold degeneracy for the rest. Thus the (200) equatorial intensity can be used to unambiguously determine the relative distribution of PPV crystallites about the equatorial plane. For the (200) equatorial profile, there are three distinct maxima in its intensity variation for χ rotations of 180°. This is indicative of a three-fold distribution of crystallites within the films. By fitting the equatorial angular distribution to a superposition of Gaussians the relative contribution of each component was estimated. The net result is that two sets of crystal planes, the [200] and [110], are preferentially oriented parallel to the film surface. These

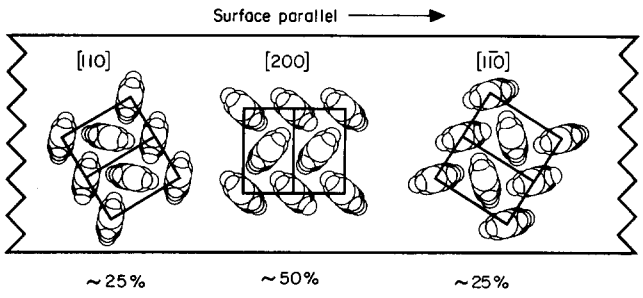

Figure 5 Schematic diagram of the preferred PPV crystallite orientation with respect to the film surface

orientation possibilities are shown schematically in *Figure 5*. A convolution of this distribution with the four-fold degeneracy of the other reflections results in calculated peak profiles similar to the experimental data, and, hence, this equatorial data is in accordance with the accepted structural model for PPV.

The precise origin of this effect has not been firmly established. If this anisotropy resulted from a combination of casting and/or surface interactions then similar anisotropy, albeit weaker, should be present and measurable in thicker film samples. PPV films ($\geqslant 10\ \mu m$) exhibited no measurable equatorial anisotropy. Thus, a more likely origin relates to the processing history. The thinnest films undergo anisotropic shrinkage during the conversion process because the web rollers only constrain the film shrinkage along (but not perpendicular to) the roller surface. Therefore, the relative reduction in film thickness is considerably greater in the direction normal to the roller surface.

The presence of this anisotropy may be considered advantageous in certain experimental situations. PPV can be doped by either electron acceptors[24] or donors[11,25] to yield highly conductive complexes. The dopant-ion diffusion induces substantial changes in the polymer chain orientations to form new structural phases. In the case of sodium metal, initial doping yields a 'hexagonal' phase (Bravais lattice) composite marked by a channel structure in which one-dimensional arrays of Na^+ ions fill columns formed by the rotation of the polymer chains about the chain axis. A (001) projection of this structure is shown in the inset of *Figure 6*. Using these equatorial anisotropic hosts it is possible to verify the dominance of simple chain axis rotations in the transformation to this phase. A contour map of the equatorial plane in a Na-doped sample (as seen in *Figure 6*) explicitly shows that the orientational ordering persists throughout the doping process and 'individual' equatorial reflections may be indexed.

The presence of equatorial anisotropy within these thin PPV films may also be relevant for studies in which thin-film samples are generally employed (e.g. electron diffraction or electron energy loss spectroscopy). The experimental data of Granier *et al.*[9] contain systematic intensity variations that would be consistent with the presence of weak equatorial anisotropy. Similarly, it is expected that other conducing polymer hosts processed from precursor films (e.g. Durham-route polyacetylene) may also fall prey to this effect.

TEMPERATURE STUDIES

We finally report on structural studies of PPV at both reduced and elevated temperatures. The primary focus for this undertaking was to correlate the systematic thermally driven changes in the projected two-dimensional unit cell. In the limiting case that PPV may be considered an example of an extended anisotropic rigid-rod rotor[26,27], the primary response on heating is for all chains to rotate and approach a so-called 'rotator' phase in which the translational and orientational symmetry of the underlying lattice is maintained but the long-range order arising from the herringbone packing of the polymer chains is lost. This property has been heavily studied in various n-alkanes[28]. As for polymers, polyethylene[29] and polyacetylene[30] both manifest subtle features of this order–disorder transition. Since PPV is stable at temperatures of up to 400°C, this would permit a wider range of study.

Alternatively, there may be local degrees of freedom that dominate. For example, phenyl-ring librational motions may arise, subject to the steric packing constraints that enforce planarity and the opposing repulsive nature of the vinyl–phenyl H–H interaction. In support of this response are temperature-dependent n.m.r. studies of partially labelled PPV samples[31] that have identified dramatic librational and ring-flip motions with an Arrhenius behaviour. Analogous results have been reported for other linear polymers, conducting[32] or otherwise[33].

In *Figure 7* the relative lattice constant shifts, as a function of temperature, are plotted. For host compounds in which the transformation to the rotator phase dominates (i.e. polyethylene or polyacetylene), the overall lattice expansion is highly anisotropic with the final high-temperature equatorial lattice constant ratio, $a/(b \sin \alpha)$, approaching a limiting value of $\sqrt{3}$. For PPV samples, the temperature-dependent response differs

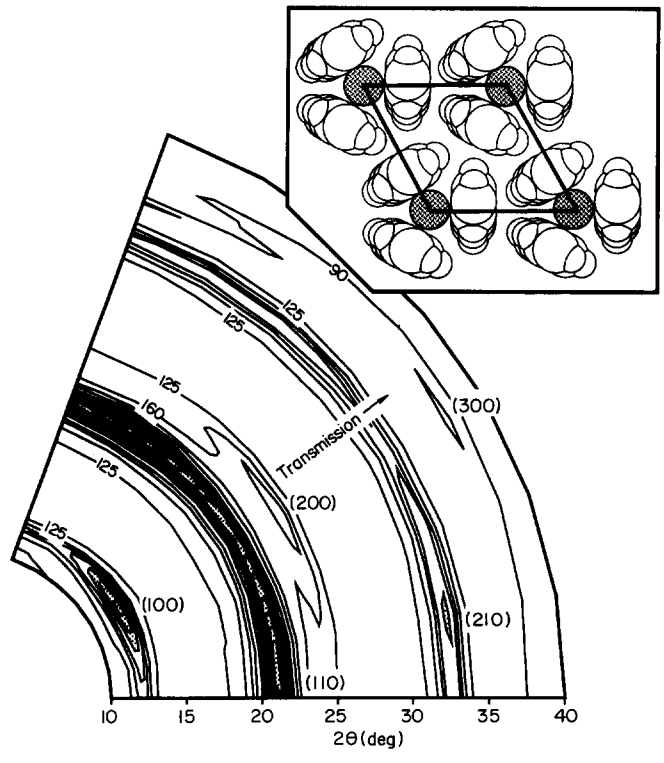

Figure 6 Constant X-ray intensity contour maps for the (*hk*0) equatorial plane of three-dimensional textured PPV films after vapour doping by sodium. Inset: equatorial projection of proposed high-symmetry hexagonal channel structure for sodium-doped PPV from reference 11

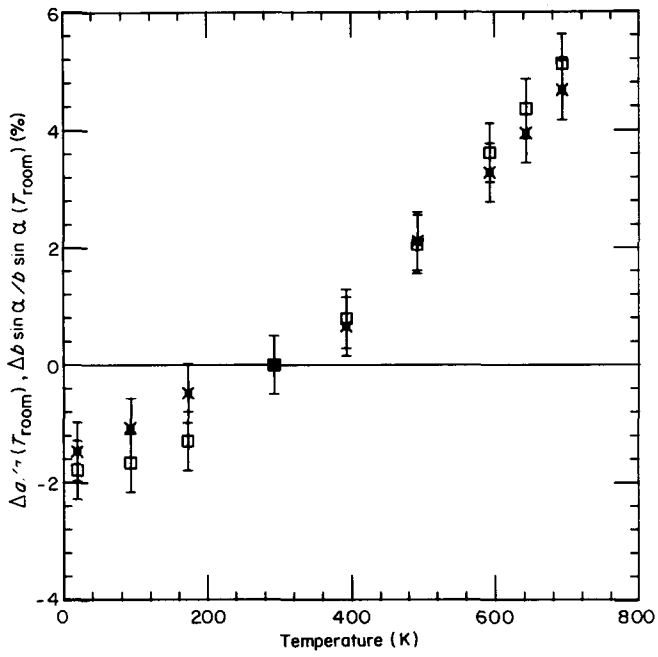

Figure 7 Graph of the relative equatorial lattice constant variations of a (×) and $b \sin\alpha$ (□) on thermal cycling

Table 2 PPV thermal parameters at representative temperatures for the sample in *Figure 2A*

Temperature (°C)	Temperature coefficient (nm^2)	Dihedral angle (deg)	Librational parameter (deg)
20	0.14	8	9
200	0.19	9	12
400	0.21	13	18

significantly with a lattice expansion that is weakly anisotropic. Thus the lattice ratio remains very close to its room temperature value of 1.58. This result tends to rule out the possibility of a transformation to a rotator phase.

In contrast, structure factor refinements to the experimental data strongly support a model in which there are local phenylene ring motions that are thermally activated. Detailed analysis of the most intense ($hk0$) scattering features shows systematic changes in the measured peak intensities that cannot be accounted for by a gradual increase in an isotropic equatorial temperature factor (which simply introduces a monotonic exponential decrease of the measured peak intensity at higher angles). These observed intensity variations are better accommodated by assuming an increasing θ_D combined with more pronounced librational motions as the temperature increases to 400°C. Estimates of these parameters are displayed in *Table 2**. Hence, our results clearly support a model requiring phenyl ring motions in a double-well potential. This result is not only in agreement with the aforementioned n.m.r. findings but is also in accordance with i.r. dipole studies by Bradley[4] that are suggestive of a non-planar conformation. We also note that molecular stilbene is, in essence, only partially representative of the true intrachain interactions in PPV, for there is only a single repulsive vinyl–phenyl H–H interaction per phenyl ring in stilbene as compared to twice that in the actual polymer.

Since the X-ray scattering has strong contributions by carbon atoms close to the polymer chain axis centres, a comprehensive analysis of the librational motion was not undertaken. Given the exceptional structural characteristics present in PPV films combined with the neutron's sensitivity to various hydrogen isotopes, a neutron scattering study of PPV may be able to provide definitive and direct measures for both the orientation and thermal response of the phenylene units. In terms of specific electronic properties, PPV is striking for it exhibits a π–π^* interband transition energy $\sim$0.3 eV larger than for either alkyl or alkoxy side-chain substituted homologues[34]. While this difference can be accounted for by variations in the electron-withdrawing capabilities of the side groups, a non-planar conformation of the phenyl rings should be responsible for some fraction of this difference. Moreover, n.m.r. studies of doped PPV compounds would yield information concerning the doping-induced bonding reconfigurations[35]. The charge-transfer process which accompanies doping promotes the development of π-bonding across the vinyl–phenyl C–C linkage. Hence, there should be a reduction or even an elimination of the large-scale ring motions. This behavioural response has already been reported in protonated polyaniline films[32], a conjugated polymer with significantly less crystalline perfection[36].

CONCLUSIONS

The results presented in this paper support the previously proposed PPV structural model but with notable exceptions. Our improved refinements indicate that ϕ_s is closer to 50° and that PPV adopts a non-planar conformation with a θ_D that exceeds 10°. Temperature-dependent studies demonstrate that local degrees of freedom dominate the thermal response of PPV and that significant phenylene ring librations are generated. In addition, we find that certain PPV samples exhibit pronounced structural complications. The presence of these is manifested in the X-ray diffraction profiles as equatorial anisotropy and as unusually small ϕ_s values. There is, at present, only preliminary evidence suggesting that these effects are related to the specific details of the polymer processing history.

ACKNOWLEDGEMENTS

We are grateful for financial support from the University of Wisconsin and NSF DMR Grant no. DMR-8917530 (DC and MJW), from the AFOSR (MAM and FEK) and jointly from DARPA-AFOSR. We would also like to thank D. M. Rice for communicating his n.m.r. results prior to publication.

REFERENCES

1 Kanbe, M. and Okawara, M. *J. Polym. Sci. A1* 1968, **6**, 1058
2 Wessling, R. A. and Zimmerman, R. G. *US Pat. 3 401 152*, 1968
3 Edwards, J. H. and Feast, W. J. *Polym. Commun.* 1989, **21**, 595
4 Bradley, D. D. C. *J. Phys. D* 1987, **22**, 1389

*There is considerable uncertainty in the absolute magnitude of these parameters for there is discretion (e.g. choice of an isotropic temperature factor or the explicit form of the Lorentz factor) in selecting an appropriate parameterization. For further details refer to reference 18

5 Bradley, D. D. C., Friend, R. H., Hartmann, T., Marseglia, E. A., Sokolowski, M. M. and Townsend, P. D. *Synth. Met.* 1987, **17**, 473
6 Gagnon, D. R., Karasz, F. E., Thomas, E. L. and Lenz, R. W. *Synth. Met.* 1987, **20**, 85
7 Moon, Y. B., Rughooputh, S. D. D. V., Heeger, A. J., Patil, A. O. and Wudl, F. *Synth. Met.* 1989, **29**, E79
8 Bradley, D. D. C., Hartmann, T., Friend, R. H., Marseglia, E. A., Linenberger, H. and Roth, S. 'Electronic Properties of Conjugated Polymers', Vol. 76, Springer Verlag, Berlin, 1987, p. 308
9 Granier, T., Thomas, E. L., Gagnon, D. R., Lenz Jr, R. W. and Karasz, F. E. *J. Polym. Sci., Polym. Phys. Edn* 1986, **24**, 2793
10 Granier, T., Thomas, E. L. and Karasz, F. E. *J. Polym. Sci., Polym. Phys. Edn* 1988, **26**, 65
11 Chen, D., Winokur, M. J., Masse, M. and Karasz, F. E. *Phys. Rev. B* 1990, **41**, 6759
12 Masse, M. A. *PhD Thesis* University of Massachusetts, 1989
13 Gagnon, D. R., Capistran, J. D., Karasz, F. E., Lenz, R. W. and Antoun, S. *Polymer* 1987, **28**, 567
14 Machado, J. M., Karasz, F. E., Kovar, R. F., Burnett, J. M. and Druy, M. A. *New Polym. Mater.* 1989, **1**, 189
15 Smith, P. J. C. and Arnott, S. *Acta Cryst. A* 1976, **34**, 3
16 Finder, C. J., Newton, M. G. and Allinger, N. L. *Acta Cryst. B* 1974, **30**, 411
17 Cailleau, H., Baudour, J.-L., Meinnel, J., Dworkin, A., Moussa, F. and Zeyen, C. M. E. *Faraday Disc. Chem. Soc.* 1980, **69**, 7
18 Alexander, L. E. 'X-ray Diffraction Methods in Polymer Science', Wiley, New York, 1969
19 Hosemann, R. and Bagchi, S. N. 'Direct Analysis of Diffraction by Matter', North-Holland, Amsterdam, 1962
20 Busing, W. R. *Macromolecules* 1990, **23**, 4068
21 Sun, D. C. and Magill, J. H. *J. Polym. Sci. Lett.* 1989, **27**, 65
22 Mitchell, G. R., Davis, F. J. and Legge, C. H. *Synth. Met.* 1988, **26**, 247
23 Russell, T. P. *J. Polym. Sci., Polym. Phys. Edn* 1984, **22**, 1105
24 Masse, M. A., Schlenoff, J. B., Karasz, F. E. and Thomas, E. L. *J. Polym. Sci., Polym. Phys. Edn* 1989, **27**, 2045
25 Chen, D., Winokur, M. J. and Karasz, F. E. *Synth. Met.* 1991, **41**, 341
26 Choi, H.-Y., Harris, A. B. and Mele, E. J. *Phys. Rev. B* 1989, **40**, 3766
27 Choi, H.-Y. and Mele, E. J. *Phys. Rev. B* 1989, **40**, 3439
28 Guillame, F., Doucet, J., Sourisseau, C. and Dianoux, A. J. *J. Chem. Phys.* 1989, **91**, 2555
29 Kawaguchi, A., Ohara, M. and Kobayashi, K. *J. Macromol. Sci.* 1979, **B16**, 193
30 Ma, J., Fischer, J. E., Scherr, E. M., MacDiarmid, A. G., Jósefowicz, M. E., Epstein, A. J., Mathis, C., Francois, B., Coustel, N. and Bernier, P. *Phys. Rev. B* 1991, **44**, 11609
31 Simpson, J. H., Rice, D. M. and Karasz, F. E. *J. Polym. Sci., Polym. Phys. Edn* 1992, **30**, 11
32 Kaplan, S., Conwell, E. M., Richter, A. F. and MacDiarmid, A. G. *Synth. Med.* 1989, **29**, E235
33 Cain, E. J., Gardner, K. H., Gabara, V., Allen, S. R. and English, A. D. *Proc. Am. Chem. Soc. Polym. Prepr.* 1990, 518
34 Murase, I., Ohnishi, T., Noguchi, T. and Hirooka, M. *Synth. Met.* 1987, **17**, 639
35 Skotheim, T. (Ed.) 'Handbook of Conducting Polymers', Vols 1 and 2, Dekker, New York, 1986
36 Jozefowicz, M. E., Laversanne, R., Javadi, H. H. S., Epstein, A. J., Pouget, J. P., Tang, X. and MacDiarmid, A. G. *Phys. Rev. B* 1989, **39**, 12958